



Antimicrobial Anilinium Polymers: The Properties of Poly(*N,N*-dimethylaminophenylene methacrylamide) in Solution and as Coatings

Ao Chen,^{1,2} Gerald Er,^{1,2} Cheng Zhang,^{1,2} Joyce Tang,^{1,2} Mahbub Alam,^{1,2} Hang T. Ta,^{1,2} Alysha G. Elliott,³ Matthew A. Cooper,³ Janesha Perera,⁴ Simon Swift,⁴ Idriss Blakey,^{1,5} Andrew K. Whittaker ^{1,2}, Hui Peng ^{1,2}

¹Australian Institute for Bioengineering and Nanotechnology, The University of Queensland, Brisbane, Queensland 4072, Australia

²Australian Research Council Centre of Excellence for Convergent Bio-Nano Science and Technology, Brisbane, Queensland 4072, Australia

³Institute for Molecular Bioscience, The University of Queensland, Brisbane, Queensland 4072, Australia

⁴Faculty of Medical and Health Sciences, Department of Molecular Medicine and Pathology, University of Auckland, Auckland 2013, New Zealand

⁵Centre for Advanced Imaging, The University of Queensland, Brisbane, Queensland 4072, Australia

Correspondence to: A. Whittaker (E-mail: a.whittaker@uq.edu.au) or H. Peng (E-mail: h.peng@uq.edu.au)

Received 31 October 2018; accepted 13 December 2018

DOI: 10.1002/pola.29314

ABSTRACT: Antimicrobial polymers have been widely reported to exert strong biocidal effects against bacteria. In contrast with antimicrobial polymers with aliphatic ammonium groups, polymers with anilinium groups have been rarely studied and applied as biocidal materials. In this study, a representative polymer with aniline side functional groups, poly(*N,N*-dimethylaminophenylene methacrylamide) (PDMAPMA), was explored as a novel antimicrobial polymer. PDMAPMA was synthesized and its physicochemical properties evaluated. The methyl iodide-quaternized polymer was tested against the Gram-positive *Staphylococcus aureus*, with a minimum inhibitory concentration (MIC) and minimum bactericidal concentration (MBC) of 16–32 and 64–128 $\mu\text{g mL}^{-1}$, respectively. Against the Gram-negative *Escherichia coli*, the MIC and MBC were both

64–128 $\mu\text{g mL}^{-1}$. To broaden the range of applications, PDMAPMA was coated on substrates via crosslinking to endow the surface with contact-kill functionality. The effect of charge density of the coatings on the antimicrobial behavior was then investigated, and stronger biocidal performance was observed for films with higher charge density. This study of the biocidal behavior of PDMAPMA both in solution and as coatings is expected to broaden the application of polymers containing aniline side groups and provide more information on the antimicrobial behavior of such materials. © 2019 Wiley Periodicals, Inc. *J. Polym. Sci., Part A: Polym. Chem.* **2019**

KEYWORDS: biological applications of polymers; biomaterials; surfaces

INTRODUCTION While bacteria are often beneficial to humans, they can also cause serious infections. The World Health Organization has found that 7% of patients in developed countries and 10% in developing countries will acquire at least one health care-associated infection at any given time.¹ The overuse of antibiotics has exacerbated this situation, and led to the evolution of antibiotic-resistant organisms. It was estimated that more than 700,000 deaths were caused by antibiotic-resistant bacterial strains in 2010 and that number is expected to surpass 10 million in 2050.² Bacterial resistance to antibiotics can be acquired through four principal mechanisms: (a) enzymatic inactivation or modification of the chemical structure of the antibiotics; (b) alteration of the structure

of the binding sites; (c) alteration of the metabolic pathways to avoid the antibiotics; and (d) reduction of the accumulation of antibiotics through changes in the permeability of cell membranes.³ Such mutations call for the development of antibiotics which exploit different mechanisms of action against bacteria.

It is known that natural host defense peptides, for example, magainin, α - and β -defensins,⁴ are able to kill bacteria by taking advantage of the net negative charge of the cell membrane and by acting as surfactants by virtue of their amphiphilic character.^{5,6} This mechanism of action significantly slows down the development of resistance against antibiotics.⁶

Additional supporting information may be found in the online version of this article.

© 2019 Wiley Periodicals, Inc.

However, the synthesis of host defense peptides requires extensive expertise and large financial investment. Antimicrobial polymers, which mimic the structure and function of host defense peptides,⁷ have been shown to possess moderate to high biocidal activity against bacteria.⁷ The poly(quaternary ammonium salt)s (polyQAS) is the most widely explored antimicrobial polymers. The most commonly used active moieties of polyQAS are listed in Scheme 1. However, as an important member of this class of structures, quaternary anilinium groups have not been widely tested. Two studies of polymers using this active functionality are known by us. Ortega et al.⁸ prepared and studied anilinium-terminated carbosilane dendrimers and showed that they were effective against *Staphylococcus aureus* and *Escherichia coli*. Very recently, Tolosa et al.⁹ examined the biocidal activity of poly(phenylene)vinylene derivatives with different geometries and peripheral functional groups, including the aniline derivatives. These latter compounds only exhibit moderate activity; however, these two reports demonstrate the importance of multivalence and provide sufficient motivation for further exploration of the biocidal behavior of anilinium-containing macromolecules.

Aniline, an important member of the family of aromatic amines, has been the basis of the synthetic dye industry, and is frequently utilized in the field of rubber additives and as precursors for the synthesis of several important drugs, such as paracetamol.¹⁰ Aniline can also act as a monomer in the synthesis of the conductive polymer polyaniline. In its neutral state, aniline is highly hydrophobic, but is water soluble if protonated.¹⁰ Therefore, aniline is soluble in water after quaternization. The conjugation of amine and benzene groups leads to a planar spatial structure and strong delocalization of electrons, which reduces the electron density on the amine group and reduces its basicity.¹⁰ Such a structure also provides a large steric hindrance when used as a side group to the main chain, and shifts the amphiphilic balance of the antimicrobial polymer toward high hydrophobicity, which is crucial for biocidal performance and cytotoxicity.¹¹ Based on these properties, significant biocidal behavior is expected for antimicrobial polymers with quaternary anilinium groups.

Poly(*N,N*-dimethylaminophenylene methacrylamide) (PDMAPMA) is a representative polymer with pendant anilinium groups. Its monomer *N,N*-dimethylaminophenyl methacrylamide (DMAPMA)¹² and its polymer¹³ were first synthesized by Sokolova and Ovsyannikova in the late 1950s. About 30 years later, Li et al. investigated the effect of different initiators on the polymerization of this monomer.¹⁴ Not until the 2000s did Liaw et al.^{15,16} examine the copolymerization of DMAPMA with methacrylamide,

and the properties of the quaternary and zwitterionic derivatives of PDMAPMA in water. These authors did not examine the antimicrobial properties of their polymers. To our knowledge, no further studies or applications of this polymer have been reported.

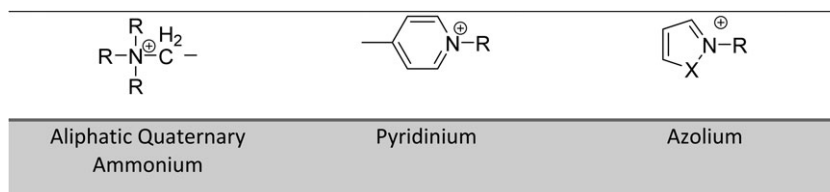
In this article, the properties of PDMAPMA prepared through free-radical polymerization are reported in detail. The static and dynamic antimicrobial action of the homopolymer quaternized with methyl iodide was thoroughly investigated through measurement of minimum inhibitory/bactericidal concentrations (MIC, MBC) and time-kill curves against common pathogens. Furthermore, coatings of PDMAPMA on solid substrates were fabricated to broaden the range of applications of this material. The coatings were prepared through dip coating onto silicon wafers, crosslinking, and quaternization of the polymers and then tested against *S. aureus* and *E. coli* to study the efficiency of contact killing. The effect of charge density on the biocidal effectiveness of the coatings was also investigated by varying the degree of quaternization. This study is expected to broaden the application of polymers with aniline as functional side groups in the field of antimicrobial polymers and provide more information on the antimicrobial behavior of such material.

EXPERIMENTAL

Materials

The main raw materials for the syntheses of monomer DMAPMA and polymer PDMAPMA, that is, *N,N*-dimethyl-1,4-phenylene diamine, methacryloyl chloride and 2,2'-azobis(2-methylpropionitrile) (AIBN), were purchased from Sigma Aldrich St. Louis, Missouri, United States. AIBN was recrystallized from ethanol before use. *N,N*-dimethylformamide (DMF) and dichloromethane (CH₂Cl₂), were purified in an MBRAUN Solvent Purification System. Tetrahydrofuran (THF), hexane, ethyl acetate, diethyl ether, and *N,N*-dimethylacetamide (DMAc) in high-performance liquid chromatography (HPLC) grade were provided by Merck. Dimethyl sulfoxide (DMSO) in analytical grade was purchased from Chemical-Supplies. Deuterated DMSO (DMSO-*d*₆) for nuclear magnetic resonance (NMR) sample preparation was supplied by Cambridge Isotope Laboratories. Methyl iodide, sodium chloride, sodium hydroxide, and sodium sulfate were supplied by Chemical-Supplies. The crosslinker 1,4-dibromobutane was provided by Sigma.

For the biocidal assays, *S. aureus* (ATCC 25923) and *E. coli* (ATCC 25922) were used as representative bacterial strains. Mueller-Hinton broth (MH Broth) was provided by OXOID. Nutrient agar was purchased from Merck. Phosphate-buffered



SCHEME 1 The structure of typical quaternary ammonium groups of antimicrobial polyQAS.

saline (PBS) was prepared by dissolving PBS tablets (Amresco) in reverse osmosis water (one tablet/100 mL). The above growth media were sterilized by autoclaving at 121 °C for 20 min and used within 1 month. Live/dead BacLight stain was purchased from Thermo Fisher and prepared according to the method provided by the supplier. Then, 25% glutaraldehyde and hexamethyldisilazane (HMDS) for sample preparation for scanning electron microscopy (SEM) were provided by Chem-Supply. The glutaraldehyde solution was diluted into 2.5% using PBS and stored at 4 °C before use.

For the cytotoxicity tests, Dulbecco's Modified Eagle Medium (DMEM) was provided by Thermo Fisher. The cells tested were NIH/3T3 (ATCC CRL-1658) fibroblast cells. For hemolysis tests, fresh human red blood cells (RBCs) were used.

Methods of Characterization

Characterization of Polymers in Solution

Nuclear Magnetic Resonance

Proton and carbon NMR spectra (^1H NMR and ^{13}C NMR spectra) were acquired on a Bruker ASCEND 400 MHz NMR spectrometer operating at 400.13 MHz. Other parameters for ^1H NMR spectra were set as follows: number of scans: 64; acquisition time: 4.085 s; and temperature 300.0 K. The parameters for ^{13}C NMR spectra were number of scans: 6000; acquisition time: 1.486 s; and temperature 300.0 K. All samples were prepared by dissolving in $\text{DMSO-}d_6$ and referenced to the residual DMSO at a chemical shift at 2.5 ppm for the ^1H NMR spectra and 39.53 ppm for the ^{13}C NMR spectra.

Size Exclusion Chromatography

The molecular weight distributions of the polymers were measured on a Polymer Labs GPC50 system consisting of two PLGel Mixed B (7.8 × 300 mm) size exclusion chromatography (SEC) columns connected in series. HPLC-grade DMAc with 0.03 wt % LiCl was used as the eluent at a flow rate of 1.0 mL min^{-1} . The injection volume was set at 100 μL and run time to 30 min at a constant temperature of 50 °C. The SEC was calibrated using standard PS samples. The SEC samples were prepared by dissolving the polymer in DMAc (containing LiCl) at a concentration of around 2 mg mL^{-1} and filtered through a 0.45 μm filter.

Differential Scanning Calorimetry and Thermogravimetric Analysis

The glass transition temperature (T_g) and thermal decomposition of the polymer were measured on a Mettler Toledo differential scanning calorimetry (DSC)/thermogravimetric analysis (TGA; STARE) system. DSC samples were prepared by weighing about 5 mg of the polymer in a standard 40 μL aluminum pan. The heating rate was set at 10 °C min^{-1} and two cycles of heating from 30 to 250 °C were performed under nitrogen atmosphere with a flow rate of 15 mL min^{-1} . The T_g reported here was measured on the second heating run. For TGA measurements, around 10 mg of sample was weighed in a 70 μL alumina pan and heated from 25 to 700 °C at a rate of 10 °C min^{-1} in a nitrogen atmosphere.

pH Responsiveness and Ultraviolet-Visible Spectra

Total of 20 mg polymer was dissolved in 2 mL HCl with a pH value of 0.5 to make a 10 mg mL^{-1} solution. In the meantime, a series of buffers with pH ranging from 2.2 to 8.0 was prepared from 0.1 mol L^{-1} citric acid and 0.2 mol L^{-1} Na_2HPO_4 aqueous solution according to a previously reported protocol.¹⁷ All solutions, including the polymer solution, were filtered through 0.45 μm syringe filters to remove undissolved particles before use.

In a plastic cuvette, 1 mL of buffer and then 0.1 mL of polymer solution were added and thoroughly mixed. The transmittance of the solution was measured on a Varian Cary 4000 ultraviolet-visible (UV-Vis) Spectrophotometer from 400 to 700 nm. For each sample, three measurements were made to calculate an average value.

The UV spectra were also measured on the Varian Cary 4000 UV-Vis Spectrophotometer. Quartz cuvettes were used with all substances dissolved in THF. The spectra were measured over a wavelength range of 200–800 nm.

Characterization of Films

Contact Angle Measurements

Static contact angles were measured using a Data Physics Instruments Optical Contact Angle Series 5 goniometer. The contact angles reported here were measured by the addition of a 5 μL drop of water at two different locations for each thin film and a triplicate of measurements for each type of film was conducted.

X-ray Photoelectron Spectroscopy

The nitrogen 1S spectra of the coatings were measured using X-ray photoelectron spectroscopy (XPS) to characterize the degree of quaternization on a Kratos AXIS Ultra spectrometer (Kratos Analytical, Manchester, UK) with a 165 mm hemispherical electron-energy analyzer and monochromatic AlK α X-ray source (1486.6 eV) operating at 300 W (15 kV, 20 mA). The XPS spectra were analyzed using CasaXPS version 2.3.12 software. The N1s spectra were rescaled to 399.7 eV to compensate for charging effects.

Spectroscopic Ellipsometry

Thicknesses of the films after annealing were measured on a J.A. Woollam VASE ellipsometer. Thin film samples were scanned using polarized light with a wavelength from 300 to 800 nm at incidence angles of 55, 60, 65, 70, and 75°. The thicknesses of the films were obtained by fitting the data using WVase32 software.

Surface Streaming Potential

The streaming potentials of the films were measured using an Anton Paar SurPASS electrokinetic analyzer. For each type of films, two planar samples with a size of 20 × 10 mm were loaded in the adjustable gap chamber. The two samples were aligned in parallel facing each other with a ~100 μm gap to form a microchannel. Total of 1 mM KCl was used as the electrolyte solution and pumped through the microchannel at

0–300 mbar. The streaming potential of the coatings was calculated from the streaming current using the Helmholtz–Smoluchowski equation. Each streaming potential was measured four times and the average value was taken.

Synthesis of Monomers and Polymers

Synthesis of DMAPMA Monomer

DMAPMA monomer was prepared following a procedure adapted from a previous report.¹⁵ *N,N*-dimethyl-1,4-phenylene diamine (5.05 g, 0.0367 mol) was dissolved in CH₂Cl₂ (36.7 mL) and the solution was mixed with 6 mol L⁻¹ NaOH aqueous solution (9.18 mL) in a 250 mL three-necked flask. The flask was sealed and purged with argon for 10 min. Methacryloyl chloride (3.9 mL, 0.0404 mol) was diluted in 3.42 mL CH₂Cl₂ and added dropwise into the solution, with the temperature of the solution maintained below 10 °C using an ice bath. After the addition of methacryloyl chloride, the solution was kept stirring at room temperature for another 6 h.

Milli-Q water was added to quench the unreacted methacryloyl chloride. The organic phase was separated, washed with Milli-Q water until the aqueous phase was neutral and then with saturated brine once. The organic phase was dried over anhydrous Na₂SO₄ and the solvent was evaporated to obtain the crude product. The crude product was recrystallized three times using ethyl acetate and hexane with a volumetric ratio of 1:3. Needle-like crystals of dark brown color were acquired. The yield was calculated to be 91.4%. The structure of the product was confirmed through ¹H NMR spectroscopy [Fig. 1(A)].

Synthesis of Polymer PDMAPMA

Polymer PDMAPMA was synthesized using free-radical polymerization. DMAPMA (1.5 g, 7.34 mmol) and AIBN (12.0 mg, 0.0734 mmol) were mixed with DMF (3 mL) in a 25 mL round-bottom flask equipped with a magnetic stir bar and sealed with a Suba seal. The solution was purged with argon for 30 min and then immersed in an oil bath thermostated at 70 °C for 24 h. Conversion of the monomer to polymer was calculated from ¹H NMR to be 92.9%. The product PDMAPMA was collected by precipitating the solution into cold diethyl ether and then from THF to hexane to afford a gray powder. The final product was dried under vacuum, with a yield of 1.3 g.

Quaternization of the Polymer

Total of 0.1 g of the polymer was dissolved in 2 mL DMSO. Quaternization of PDMAPMA was conducted by adding methyl iodide (0.328 mL, 5.27 mmol) into the polymer solution. The solution was stirred at 60 °C for 24 h in darkness. The polymer was purified by precipitation into THF and dialysis against water. Quaternized polymer MeI-PDMAPMA was collected through lyophilization.

Fabrication of Coatings

Dip Coating of PDMAPMA

Silicon wafers were cut into 1 cm × 1 cm size and cleaned by sonication in acetone and then isopropanol for 10 min each. The wafers were blown dry and baked at 150 °C to remove

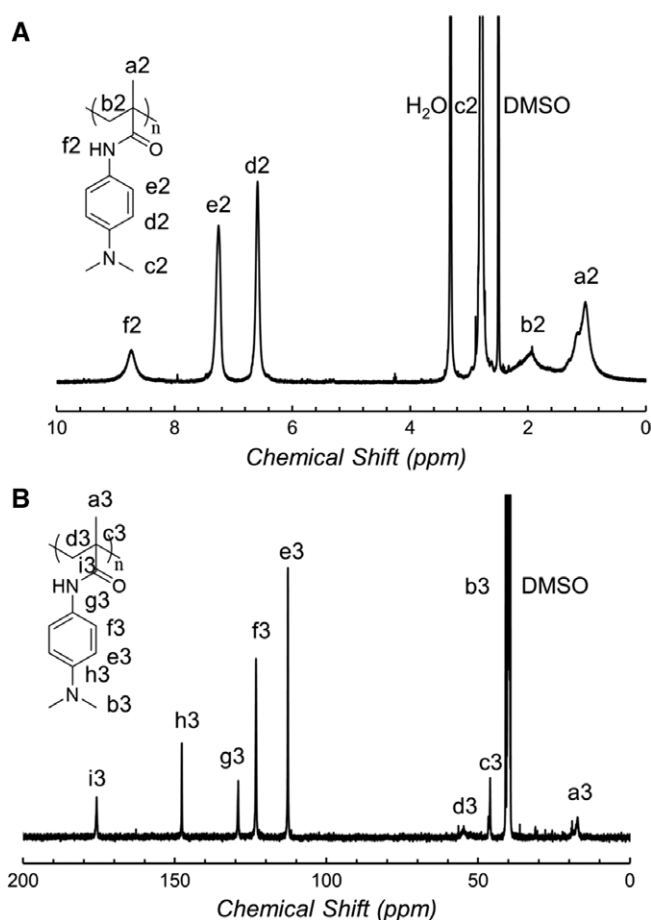


FIGURE 1 NMR spectra of polymer PDMAPMA in DMSO-*d*₆. (A) ¹H NMR spectrum of PDMAPMA. (B) ¹³C NMR spectrum of PDMAPMA.

the residual solvent. A 5 mg mL⁻¹ solution for dip coating was freshly prepared by adding PDMAPMA into a mixed solvent of THF and 1,4-dibromobutane with a volumetric ratio of 80:20. The solution was mixed thoroughly on a vortex and filtered through 0.22 μm filters before use.

PDMAPMA films were fabricated by dip coating the wafers into the PDMAPMA solution at a rate of 4 cm min⁻¹. The samples were then baked at 60 °C for 24 h in a nitrogen atmosphere to allow crosslinking. Finally, samples were thoroughly rinsed with THF to remove uncrosslinked PDMAPMA and unreacted 1,4-dibromobutane, and dried under vacuum.

Quaternization of PDMAPMA Films

The above crosslinked films were submerged in methyl iodide solution in THF. The reaction time and the amount of methyl iodide were varied to control the degree of quaternization of the films. After quaternization, the coatings were removed from the solution and thoroughly rinsed with THF to wash unreacted methyl iodide. Three types of films of different degree of quaternization were fabricated, namely films quaternized by only crosslinking (PDMAPMA-Crosslinked), films with a middle degree of quaternization (PDMAPMA-Mid QAS),

and films with a high degree of quaternization (PDMAPMA-High QAS).

Biological Assays

Tests of PDMAPMA in Solution

MIC Assays of MeI-PDMPMA

A microdilution method used for measurement of the MIC was adapted from a previously reported protocol.¹⁸ Briefly, a stock solution of MeI-PDMPMA was prepared by dissolving the polymer in sterile MH broth with a concentration of 4 mg mL⁻¹ and was further serially diluted twofold across the wells on a polypropylene 96-well plate using fresh broth, with concentrations ranging from 8 μg mL⁻¹ to 4 mg mL⁻¹, plated in triplicate. A culture of bacteria was inoculated in 2 mL fresh MH broth from independent colonies grown overnight at 37 °C on nutrient agar. The suspension was adjusted until the bacterial density reached 1 × 10⁸ colony-forming units (cfu mL⁻¹). The culture was further diluted using fresh MH broth to 1 × 10⁶ cfu mL⁻¹. Total of 50 μL of the diluted culture was then added to each well of the polymer-containing 96-well plate, with a final cell density of 5 × 10⁵ cfu mL⁻¹ and concentration of the polymer ranging from 4 to 2 μg mL⁻¹. Two columns of the 96-well plate were, respectively, kept as the growth control of the culture and the negative control of the sterile broth. The plates were covered and incubated at 37 °C for 18 h. MICs were determined visually, being defined as the lowest concentration showing no visible growth. A duplicate of independent experiments was conducted.

MBC Assays of MeI-PDMPMA

MBC tests were conducted only for MeI-PDMPMA. The above suspensions after MIC measurement were incubated at 37 °C for an additional 4 h. Total of 100 μL of visually clear wells was withdrawn and spread on nutrient agar plates. The plates were incubated at 37 °C overnight and the colonies were counted. The MBC is defined as the lowest concentration to kill >99.9% bacterial cells, that is, <50 cfu on the agar plates.

Time-Kill Curves of MeI-PDMPMA

A stock solution of MeI-PDMPMA was prepared by dissolving the polymer in sterile MH broth to achieve a concentration of 4 mg mL⁻¹. A bacterial culture of 1 × 10⁶ cfu mL⁻¹ was also prepared using the method described above. Then, 21.70 mL MH broth, 2.5 mL of bacterial culture, and 800 μL of polymer solution were mixed in a 50 mL centrifuge tube to reach 128 mg mL⁻¹ (MBC) MeI-PDMPMA and 1 × 10⁵ cfu mL⁻¹ and incubated at 37 °C while agitated at 200 rpm, with bacterial suspension without the polymer as control. Total of 100 μL of the suspension was removed and serially diluted 10-fold for spreading on agar plates at 0, 1, 2, 4, 6, and 8 h of incubation. The plates were incubated at 37 °C overnight to count the cfu. Two independent replicates of the assay were conducted.

Hemolysis Assays of MeI-PDMPMA

Blood from healthy volunteers taking no medication was collected and anticoagulated with citric acid. RBCs were pelleted by centrifuging 1 mL of blood and washed three times with

PBS. PBS was added into the pelleted RBCs until a volume of 1 mL was reached. Total of 0.5 mL RBCs was resuspended in 9.5 mL PBS. MeI-PDMPMA stock solution with a concentration of 20 mg mL⁻¹ was prepared by dissolving the polymer in PBS and a series of concentrations from 20 μg mL⁻¹ to 20 mg mL⁻¹ were prepared by dilution using PBS. Total of 50 μL of polymer solution was added to 50 μL diluted RBC solution in a round-bottom 96-well plate and the mixture was incubated at 37 °C with shaking for 1 h. The final highest concentration of polymer was 10 mg mL⁻¹. Triton X-100, a surfactant known to lyse RBCs was used as the positive control. Then, 50 μL of 0.4% Triton was added to 50 μL diluted RBC solution and incubated as above. PBS was used as the negative control. The microplate was then centrifuged at 3000g for 10 min at room temperature. The supernatants were subsequently transferred to a clean flat-bottom 96-well plate. The absorbance of the free hemoglobin was measured at 415 nm on a microplate reader. Absorbance of the series of polymer solutions was also measured. The percentage of hemolysis was calculated relative to the positive hemolysis control (Triton X-100), using the following eq 1.

$$\% \text{Hemolysis} = \frac{A - A_0 - A_P}{A_L - A_0} \times 100\% \quad (1)$$

Here, A , A_0 , A_L , and A_P are, respectively, the absorbance of sample, negative control, positive control, and polymer solution. A triplicate of experiments was performed.

Cytotoxicity Tests of MeI-PDMPMA

The cytotoxicity of MeI-PDMPMA was evaluated using 3T3 fibroblast cells through a 3-(4,5-dimethylthiazol-2-yl)-5-(3-carboxymethoxyphenyl)-2-(4-sulfophenyl)-2H-tetrazolium inner salt (MTS) assay. The procedure was based on a protocol previously reported.¹⁹ Briefly, 3T3 fibroblast cells were cultured in DMEM with 10% fetal bovine serum and 1% antibiotic-antimycotic, incubated at 37 °C for 24 h with 5% CO₂. Then, 100 μL of MeI-PDMPMA in DMEM with concentrations twofold diluted from 2.048 mg mL⁻¹ to 16 μg mL⁻¹ was prepared and added across a 96-well plate. In addition, 100 μL of DMEM medium with 20,000 3T3 fibroblast cells was added into each well to reach a final volume of 200 μL with 10,000 cells per well. The cells were incubated at 37 °C for 24 h. MTS solution (10 μL) was then added into each well and the plates was incubated for another 4 h. The plate was briefly shaken and the absorbance at 490 nm of the cells treated and untreated with MeI-PDMPMA was measured using a plate reader. The concentration of MeI-PDMPMA causing 50% of cells were killed (CC₅₀) was determined.

Observation of the Change of Bacterial Morphology through SEM

A JEOL 7001F Schottky field emission SEM (was used for observing the change in integrity of the bacterial membrane before and after the treatment with MeI-PDMPMA.

Bacteria treated with or without MeI-PDMPMA were harvested and then washed three times with sterile PBS and then fixed using 2.5% glutaraldehyde PBS solution at 4 °C for 4 h.

The cells were washed with sterile PBS three times to remove residue glutaraldehyde and adhered to plastic coverslips using poly-L-lysine. The cells were then dehydrated through a series of ethanol aqueous solution with concentrations at 20, 40, 60, 80, and twice for 100%. Finally, the cells were treated with 1:1 (volumetric) HMDS:ethanol twice and dried under air. The cells were coated with 10 nm iridium before being observed under SEM with an acceleration voltage of 3 kV.

Testing of PDMAPMA Coatings

Biocidal Assays of Coatings Having Different Degrees of Quaternization

Bacteria were inoculated on nutrient agar plates and incubated at 37 °C for 24 h. Individual colonies were picked and suspended in sterile PBS until the density reached 1×10^8 cfu mL⁻¹. The suspension was further diluted 100-fold to reach 1×10^6 cfu mL⁻¹. Samples were placed into each well of a 24-well plate, with uncoated silicon wafers as the controls. Total of 1 mL of the bacterial suspension was added into the wells to submerge the films. The 24-well plate was sealed and incubated at 37 °C and agitated at 100 rpm for 6 h. After thoroughly rinsing with sterile PBS to remove the planktonic bacteria, the wafers were stained using live/dead BacLight stain according to the supplier manual and moved to a fluorescence microscope for observation. An Olympus BX61 upright metallurgical microscope equipped with a fluorescence light source was used. Live bacteria were stained by SYTO9 and excited with a bandpass filter at 470–490 nm, showing a green color. Dead bacteria cells stained with propidium iodide were excited with a bandpass filter at 530–550 nm, showing a red color. A triplicate of samples was studied and images were taken at 10 representative

points on each sample. Images of green and red channels were combined and the numbers of live and dead cells were counted using ImageJ software.

Kinetic Studies of PDMAPMA-High QAS Coatings

The biocidal efficiency of quaternized PDMAPMA coatings was monitored through a kinetic study. Following the same procedure as described above, PDMAPMA-High QAS coatings and blank silicon wafer controls were taken out, respectively, at 1, 3, and 6 h. The staining procedure described above was used to observe the ratio of live/dead cells at each time point.

Observation of Bacteria Killed by PDMAPMA Coatings through SEM

Samples were rinsed using sterile PBS. The fixation, dehydration, sputtering, and observation of the samples were conducted following the procedure described above for the bacteria killed in solution.

RESULTS AND DISCUSSION

Synthesis of PDMAPMA Polymer and Polymer Properties

Synthesis of Monomer DMAPMA

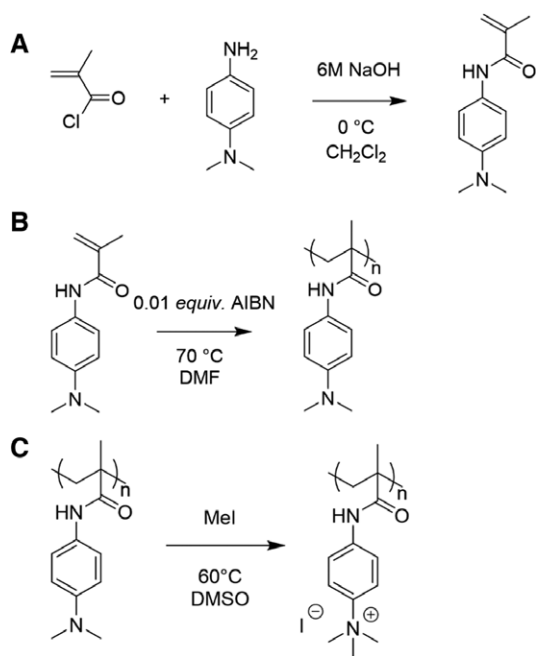
The method of synthesis of the monomer DMAPMA is shown in Scheme 2(A). A yield of 91.4% was obtained. The monomer takes the form of needle-like crystals with a dark brown color to the eye. The melting point was measured through DSC to be 131.2 °C, matching the previously reported value.¹² The ¹H NMR spectrum of the monomer DMAPMA, presented in Figure S1, confirms the structure.

Synthesis of Polymer PDMAPMA

The monomer DMAPMA was polymerized by conventional free-radical polymerization as illustrated in Scheme 2(B). The number-averaged molecular weight (M_n) was measured by SEC of DMAc solutions to be 41,400 as referred to polystyrene standards, with a molar mass dispersity of 2.1. The intended final application of the polymer is as crosslinked films, and therefore it was deemed unnecessary to prepare polymers with narrow molar mass dispersity.

The vinyl protons were consumed and their contributions to the ¹H NMR spectrum disappeared after polymerization [Fig. 1 (A)]. The peaks of the protons on the α -methyl groups shifted to around 0.8–1.5 ppm due to the consumption of the vinyl groups. Weakly resolved splitting of this resonance is due to triad tacticity. The consumption of the vinyl groups also led to a lower chemical shift of the peak due to amide protons (by around 0.7 ppm), as the delocalization effect from the vinyl group was lost. The positions of the other peaks did not change significantly. The ¹³C NMR spectrum of PDMAPMA is presented in Figure 1(B) along with the full peak assignments.

The raw material *N,N*-dimethyl phenylene diamine, monomer DMAPMA, and polymer PDMAPMA all demonstrate strong UV absorption due to the presence of the aniline structure (Fig. S2). The main absorption peak of *N,N*-dimethyl phenylene diamine appears at ~259 nm. A redshift of the main absorption peak of DMAPMA to ~273 nm was observed after



SCHEME 2 Schematic diagram of the synthesis of (A) monomer DMAPMA, (B) polymer PDMAPMA, and (C) MeI-PDMAPMA.

reaction with methacryloyl chloride, due to the strong delocalization of the conjugated structure formed by the aniline group, the amide group, and the double bond. After polymerization, a slight blue shift of the peak was observed as the vinyl group was consumed, reducing the effect of delocalization.

The thermal properties of PDMAPMA were studied using DSC and TGA. The temperature of the glass transition (T_g) of PDMAPMA was around 207 °C [Fig. S3(A)], indicative of a highly rigid structure. This is probably derived from the delocalized electron structure of the side groups, which adopt a planar arrangement and introduce steric hindrance to the main chain. In addition, PDMAPMA also has a high thermal decomposition temperature, starting at around 330 °C [Fig. S3(B)].

The pKa of PDMAPMA was measured by observing the turbidity of polymer solutions in buffers of different pH (Fig. S4). From the change of the turbidity, the pKa of the polymer is located between 4.2 and 4.4, indicating that the basicity of the aniline group is relatively weak compared to other polymers containing aliphatic amine groups. The electron withdrawal effect by the delocalized electron cloud on the benzene ring weakens the lone-pair electron on the nitrogen, further leading to the reduction in basicity of the amine groups.

Quaternization of PDMAPMA

The quaternization reaction of PDMAPMA is illustrated in Scheme 2(C). Figure 2 shows the ^1H and ^{13}C NMR spectra of PDMAPMA after quaternization by MeI.

Two sets of peaks can be seen in the ^1H NMR spectrum [Fig. 2 (A)], respectively, belonging to the unquaternized and quaternized side chains of the polymer. The quaternization of the amine group promotes the electron-withdrawal effect on the benzene ring, leading to shifts of peaks due to protons belonging to the anilinium group, c2, d2, e2, and f2 toward peaks c1, d1, e1, and f1 at higher chemical shifts. The ratio of the two sets of peaks, especially the peaks d1, e1, d2, and e2, can be used to calculate the overall extent of quaternization, as calculated using eq. 2.

$$\text{QAS\%} = \frac{I_{d1} + I_{e1}}{I_{d1} + I_{e1} + I_{d2} + I_{e2}} \quad (2)$$

The extent of quaternization was calculated to be approximately 92%. Similar changes to the chemical shifts of the peaks were also observed in the ^{13}C spectrum, as shown in Figure 2(B). After quaternization with methyl iodide, the polymer was fully soluble in water, similar to observation by Liaw et al.¹⁶ of aqueous solubility of dimethyl sulfate and propane sulfone substituted PDMAPMA.

Biocidal Behavior of MeI-PDMAPMA in Solution

The biocidal properties of PDMAPMA were tested using the microdilution method against representative Gram-positive and Gram-negative strains, *S. aureus* and *E. coli*. The antimicrobial performance was quantified as MIC and MBC values, as listed in Table 1. From the MIC value, PDMAPMA showed

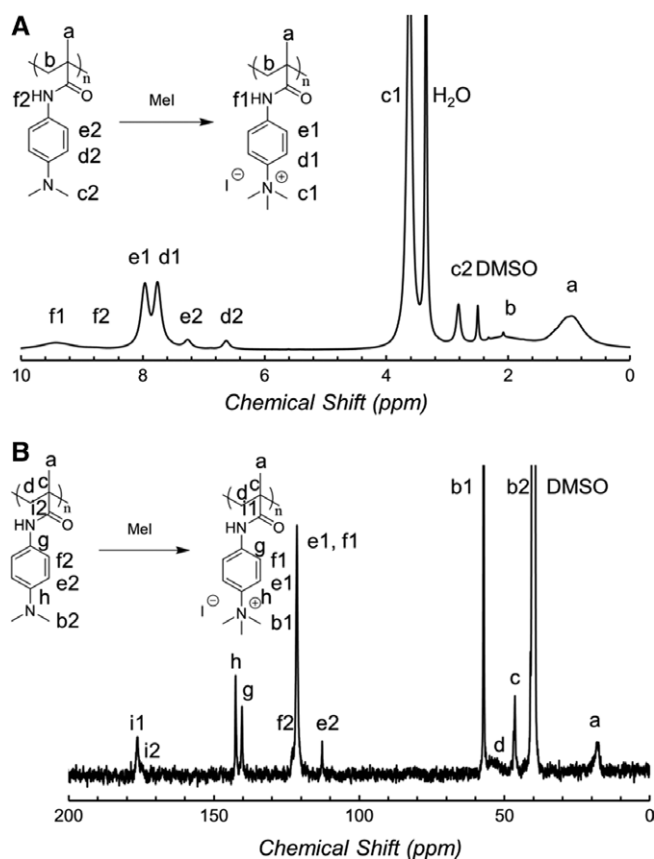


FIGURE 2 NMR spectra of MeI-quaternized PDMAPMA in DMSO- d_6 . (A) ^1H NMR of QAS-PDMAPMA. (B) ^{13}C NMR of QAS-PDMAPMA. The degree of quaternization can be calculated from ^1H NMR to be approximately 92%.

effectiveness against both *S. aureus* (16–32 $\mu\text{g mL}^{-1}$) and *E. coli* (64–128 $\mu\text{g mL}^{-1}$). A twofold to fourfold stronger inhibitory activity was detected for MeI-PDMAPMA against *S. aureus*, compared to *E. coli*. A further extension of the MIC test led to MBC values (biocidal activity) of the polymer against both strains to be between 64 and 128 $\mu\text{g mL}^{-1}$ for both strains. Against *S. aureus*, the MBC value was two to four times the MIC, while for *E. coli*, the MBC and MIC values were the same.

The lower MIC value against *S. aureus* compared to *E. coli* is consistent with studies which reported that polyQAS showed better bacteriostatic performance against Gram-positive compared to Gram-negative strains.^{20–25} Although MeI-PDMAPMA possessed a stronger inhibition effect against *S. aureus*, the same value of MBC is required for the polymer against both strains. This means that disruption of the membrane of the two strains requires the same amount of polymer in solution, that is, same intensity of interaction between the polymer and the bacteria.

To further investigate the differences in the antimicrobial actions against both bacterial strains, a kinetic study of PDMAPMA at the high end of the MBC range (128 $\mu\text{g mL}^{-1}$) was conducted. From these studies, time-kill curves of MeI-

TABLE 1 The Antimicrobial Behavior of MeI-PDMAPMA in Solution. Antimicrobial Activity of MeI-PDMAPMA against *S. aureus* and *E. coli*

Bacterial Strain	MIC ($\mu\text{g mL}^{-1}$, $\mu\text{mol L}^{-1}$) ^a	MBC ($\mu\text{g mL}^{-1}$, $\mu\text{mol L}^{-1}$) ^a
<i>S. aureus</i> (ATCC 25923)	16–32, 0.39–0.77	64–128, 1.54–3.09
<i>E. coli</i> (ATCC 25922)	64–128, 1.54–3.09	64–128, 1.54–3.09

^a The molar concentration of MIC and MBC were calculated based on the polymer molecular weight measured by SEC.

PDMAPMA at $128 \mu\text{g mL}^{-1}$ could be generated, and are shown in Figure 3. MeI-PDMAPMA started to take effect right after its addition compared to the number of live cells of the inoculum at the start of the incubation, which was set as 100%. A faster biocidal action was observed for *E. coli*, for which a sudden reduction in the numbers of live bacteria of about 1.7 orders (44–1%) occurred between 2 and 4 h of incubation. In comparison, the time-kill curve against *S. aureus* showed a slower reduction in the number of bacteria across the 8 h period, with 1% of the bacteria still left alive at the end of this period. The time-kill curves suggest that MeI-PDMAPMA has a stronger biocidal effect against *E. coli* than *S. aureus*, even though the MBC was shown to be the same for both species. This result is also contrary to the results of most previous reports, where a strain with lower MIC is associated with a faster killing rate.^{23,26,27}

Damage of the membrane structure on exposure to MeI-PDMAPMA was confirmed by SEM images of the cells before and after treatment with the polymer (Fig. 4; additional

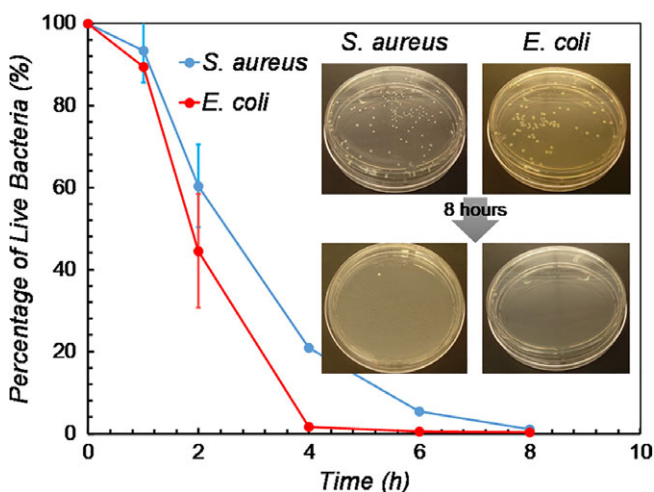


FIGURE 3 Time-kill curves of MeI-PDMAPMA at $128 \mu\text{g mL}^{-1}$ against *S. aureus* and *E. coli* over a period of 8 h. The error bars ($n = 2$) show one standard deviation. The images in the inset illustrate the reduction in number of colonies at the start and end of the 8 h incubation period. [Color figure can be viewed at wileyonlinelibrary.com]

images are presented in Fig. S5). The appearance of “blebs” on the otherwise smooth membrane of the cells demonstrates different extents of disruption to the membrane. In addition, the bacteria before treatment were well dispersed, while the dead bacteria were found clustered together. This suggests that the positively charged polymer chains exert action through adsorbing to the bacterial membrane so that independent cells adhere together to form clusters.

The observations through SEM are consistent with the mechanisms of action of host defense peptides⁶ and polyQAS proposed by Ikeda et al.,^{28,29} that polyQAS exert a biocidal effect through disruption of the bacterial membrane via electrostatic and hydrophobic interactions. This mechanism requires the adsorption of the polymer to the membrane. *S. aureus* has a thick cell wall, with a negatively charged peptidoglycan layer 20–80 nm thick covering a single cytoplasmic membrane. *E. coli* has two membranes (outer and cytoplasmic membranes), between which is a thin peptidoglycan layer of 6–8 nm thickness. It is generally accepted that *S. aureus* is more susceptible to polyQAS due to the single layer structure of the membrane and the higher negative charge.³⁰ However, the interaction between nonbiocidal moieties of the antimicrobial polymers with certain features on the bacterial membrane/cell wall may moderate biocidal activity. Such an effect was demonstrated by Punia et al.²⁶ when investigating the antimicrobial behavior of acrylic copolymers with hexamethyleneamine and poly(ethylene glycol) (PEG) side chains. The formation of hydrogen bonds between the PEG groups and the cell wall hindered the diffusion of the polymer through the cell wall. Such association of the polymer with the cell wall interfered with its interaction with the membrane, causing weaker biocidal activity against *S. aureus* than against *E. coli*. Another form of hindrance arises from the “sieving effect” proposed by Lienkamp et al.³¹ in which polymers with higher molecular weight, that is, larger size, may be blocked by the cell wall of Gram-positive bacteria, resulting in lower biocidal efficacy.

For the cationic polymer examined here, MeI-PDMAPMA, complexation with the cell wall is expected to be driven primarily by electrostatic interactions. Therefore, this property of the polymer leads to the observed differences in biocidal behavior. MeI-PDMAPMA has a relatively high molecular weight (41,400 compared to PS standards before quaternization) and bulky conjugated side groups, and therefore likely has a large size in solution and a highly rigid main chain, the latter confirmed by the high bulk glass transition temperature. Such characteristics may limit the probability of the polymer adopting specific orientations required to permit diffusion through the peptidoglycan cell wall, reducing the probability of its combination with the membrane of *S. aureus*. Thus, it is proposed that a higher concentration of polymer is needed to achieve wide-spread membrane disruption. This mechanism is similar to that underlying the “sieving effect” of cell walls, but the bacteriostatic effect of MeI-PDMAPMA at low concentrations is not affected by the hindrance to the diffusion. This suggests that interaction of MeI-PDMAPMA with *S. aureus*

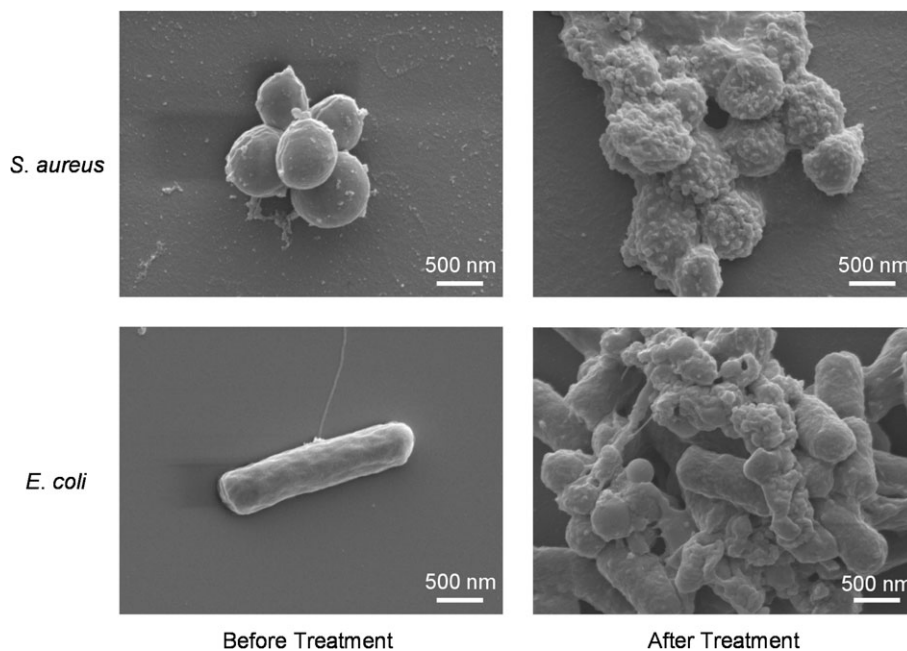


FIGURE 4 The SEM images of bacteria before and after treatment with MeI-PDMPMA. The membranes became distorted after treatment with the polymer. Bacteria were also found clustered together after treatment.

may not necessarily require fusing with the membrane. Due to the high extent of quaternization, quaternary polymers can exert strong electrostatic interactions with negatively charged bacterial membrane when immobilized on substrates or even shielded by parafilm.³² The strong electrostatic potential of MeI-PDMPMA can reach the lipid membrane when the polymer covers the negatively charged peptidoglycan cell wall, inhibiting the metabolic activity of *S. aureus*.

The Gram-negative strain, *E. coli*, has thinner cell walls, which provide much reduced hindrance toward the diffusion of MeI-PDMPMA. However, the double layers of the lipid membrane provide stronger protection of the cytoplasmic contents in the cells against polyQAS and require more intense electrostatic and hydrophobic interactions for disruption.²⁹ Such requirements are met by MeI-PDMPMA, which has a long polymer chain and high hydrophobicity. Once the forces driving polymer-cell interactions exceed the protective effect of the lipid membrane, both layers of the membrane are readily susceptible to MeI-PDMPMA and *E. coli* can be efficiently killed.

Hence, both the properties of MeI-PDMPMA and the differences in the bacterial structures lead to opposite trends in inhibition and bactericidal effects.

Biocompatibility of MeI-PDMPMA in Solution

The biocompatibility of the novel polymer MeI-PDMPMA was evaluated based on the extent of lysis of human RBCs by the polymer. MeI-PDMPMA showed $9.1 \pm 1.6\%$ hemolysis at 10 mg mL^{-1} , the highest concentration tested in this study. This indicates that MeI-PDMPMA is highly compatible with RBCs. Further biocompatibility of the polymer was assessed using 3T3 fibroblast cells. The CC_{50} was found located between 256 and $512 \text{ } \mu\text{g mL}^{-1}$, showing a mild toxicity toward human 3T3 fibroblast cells.

The selectivity of action of MeI-PDMPMA was calculated as the quotient of HC_{50} or CC_{50} and MIC or MBC, and the values are listed in Table 2. MeI-PDMPMA showed good RBC selectivity over bacteria, even at the MBC, but a relatively low

TABLE 2 The Antimicrobial Behavior of MeI-PDMPMA in Solution. Cytotoxicity and Selectivity of MeI-PDMPMA for RBCs and 3T3 Fibroblast Cells over the Two Bacterial Strains

Bacterial Strain	RBC Compatibility		3T3 Fibroblast Cell Compatibility	
	HC_{50} ($\mu\text{g mL}^{-1}$)	$>10,000$	CC_{50} ($\mu\text{g mL}^{-1}$)	256–512
	Inhibition selectivity	Bactericidal selectivity	Inhibition selectivity	Bactericidal selectivity
<i>S. aureus</i>	>312	>78	8–16	2–4
<i>E. coli</i>	>78	>78	2–4	2–4

selectivity between the bacteria and fibroblast cells, indicating a higher susceptibility of fibroblast cells from MeI-PDMAPMA.

MeI-PDMAPMA, similar to other polyQAS, kills bacteria through the disruption of the bacterial membranes. A similar mode of action applies for human cells. It has been reported that common polyQAS, such as quaternary PEIs cause cytotoxicity possibly via increasing the permeability of human cells.³³ According to previous reports on the effect of hydrophobic components of antimicrobial polymers, any factor leading to higher hydrophobicity of antimicrobial polymers not only enhances the biocidal performance of the polymer, but also increases toxicity toward mammalian cells, leading to general cytotoxicity.¹¹ The important structural factors include the length of the alkyl chain,^{31,34} the hydrophobic comonomer,³⁵ and the structure of ammonium groups.³⁶ For MeI-PDMAPMA homopolymer, no hydrophobic comonomer or long alkyl chain was introduced. In addition, a high level of quaternization was necessary to ensure water solubility of the polymer and interactions with bacteria or mammalian cells, excluding the effect of the structure of the ammonium groups. Therefore, cytotoxicity mainly derives from the overall hydrophobicity of the polymer. Increasing the hydrophilicity of the polymer by incorporating hydrophilic comonomers would likely improve the selectivity of MeI-PDMAPMA.

Fabrication of Biocidal PDMAPMA Films

Films of PDMAPMA were prepared through dip coating onto silicon wafers. In order to enhance the durability of the film in water and to avoid the dissolution of the material after further modification by methyl iodide, crosslinking of PDMAPMA through a proportion of the amine groups was conducted by reacting with 1,4-dibromobutane.^{37,38} The reaction proceeds through the same mechanism as reaction with methyl iodide, but due to the higher electronegativity of bromine compared to iodine, the leaving ability of the bromide is not as high as that of iodide.¹⁰ The reactivity of alkyl bromides to quaternize polymers with tertiary amine side functional groups (usually requires heating/reflux^{39,40}) is therefore significantly lower than that of alkyl iodide, especially methyl iodide (which readily reacts at room temperature^{8,41,42}). These observations also apply for PDMAPMA. However, alkyl bromides will still slowly react with the aniline groups in THF at room temperature and crosslinked polymer will precipitate after 2–3 days. Hence, the polymer solution should be freshly prepared before the fabrication of high quality films. After crosslinking, methyl iodide was used to quaternize the remaining amine groups of PDMAPMA and the concentration of methyl iodide and time of reaction were adjusted to achieve different degrees of quaternization of the films.

The thicknesses of the PDMAPMA-Crosslinked, PDMAPMA-Mid QAS, and PDMAPMA-High QAS films were measured through spectroscopic ellipsometry. All films had thicknesses of around 20 nm. The degree of quaternization, or the percentage of cationic amine groups, on the surface of the coatings was determined by XPS (Fig. 5). By comparing the area of the peaks in the high resolution N1s spectra at 399.7 eV

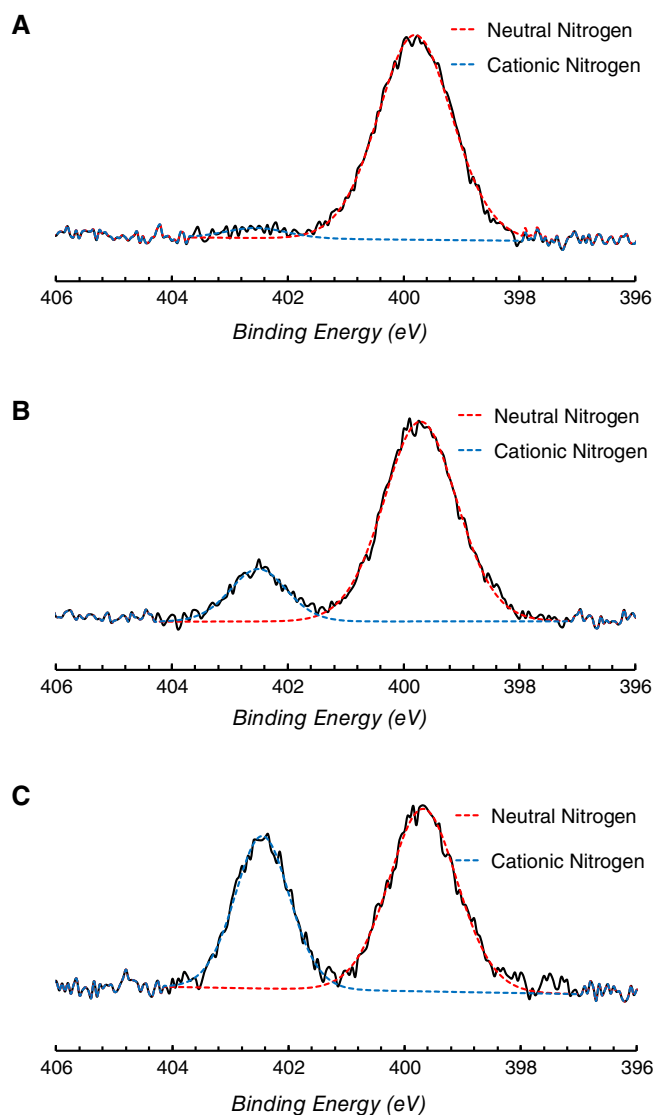


FIGURE 5 N1s XPS spectra of PDMAPMA films with different degrees of quaternization: (A) PDMAPMA films after being crosslinked by 1,4-dibromobutane (PDMAPMA-Crosslinked); (B) PDMAPMA films of middle extent of quaternization (PDMAPMA-Mid QAS); and (C) PDMAPMA films of high extent of quaternization (PDMAPMA-High QAS). [Color figure can be viewed at wileyonlinelibrary.com]

(neutral nitrogen) and 403 eV (cationic nitrogen), the degree of quaternization can be calculated, according to eq. 3:

$$\text{QAS}\% = \frac{A_{N^+}}{(A_N + A_{N^+})/2} \times 100\% \quad (3)$$

Here, QAS% is the degree of quaternization of the films, and A_N and A_{N^+} are the area of XPS peaks due to neutral nitrogen and cationic nitrogen, respectively. Since PDMAPMA has two nitrogen atoms per repeating unit, respectively, belonging to the aniline and the amide groups, the total amount of N is divided by two.

The different degrees of quaternization were accompanied by differences in charge density of the coatings. An increase in charge density promoted the polarity and subsequently the hydrophilicity of PDMAPMA, which was reflected by a decrease in water contact angle from 83 to 70° (Table 3). Accordingly, the streaming potentials of the coatings were also increased following the formation of more cationic groups on the films. For the crosslinked PDMAPMA films without quaternization, although around 8% of the amine was quaternized, the streaming potential still showed -25 mV. Since the pKa of the aniline group on PDMAPMA is between 4.2 and 4.4, the amine group was not protonated at the pH of the measurement. At this stage, the dominant number of unquaternized/unprotonated aniline groups led to an overall negative potential between the slipping layer attached to the surface and the dispersive medium. After a moderate degree of quaternization of 40% of the amine groups, the streaming potential was increased to +20 mV and a further increment was observed when the degree of quaternization reached 80%, when a value of +63 mV was achieved.

Biocidal Performance of PDMAPMA Films

Biocidal Performance of PDMAPMA with High Degree of Quaternization

The contact-killing experiments for PDMAPMA-High QAS films were conducted by incubating the films with a bacterial suspension in PBS at 37 °C for 6 h in order to better represent the everyday environment, where bacteria are in a state of low division.⁴³ The fluorescence images of the live/dead staining experiments (Figs. 6 and 7 at an incubation time of 6 h) of the PDMAPMA coatings compared to blank silicon wafers reveal that the PDMAPMA-High QAS films are highly effective against both bacterial strains.

A further test on the biocidal efficiency of PDMAPMA-High QAS was conducted through a kinetic study. The percentages of live *S. aureus* and *E. coli* attached to the films were monitored at 1, 3, and 6 h of incubation, as shown in Figures 6 and 7. The corresponding fluorescence images were presented in Figures S6 and S7.

With 100% defined as all attached cells being alive, a gradual reduction in numbers of live *S. aureus* can be seen in Figure 6 from 1 to 3 h, when around 82% of bacteria were killed. The rate of killing slowed down afterwards until 6 h, when there were 7% of live *S. aureus* left attached to the films. On the other hand, a rapid reduction in the number of live *E. coli* to 45% was seen with just 1 h of contact with the material. At 6 h,

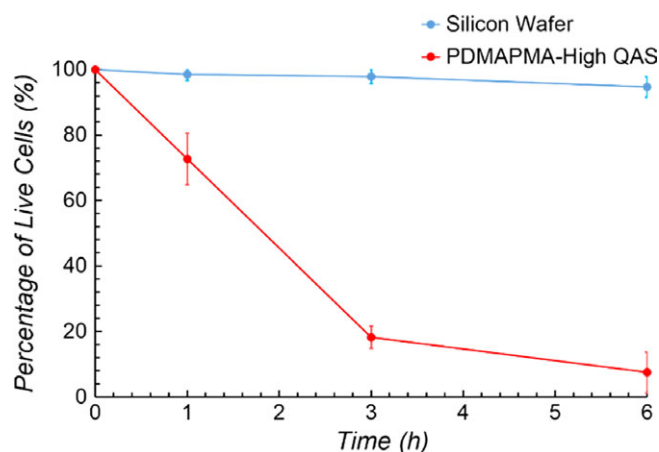


FIGURE 6 The percentage of live *S. aureus*, respectively, on silicon wafer and PDMAPMA-High QAS films as the function of incubation time at 1, 3, and 6 h. The error bars ($n = 3$) show one standard deviation. [Color figure can be viewed at wileyonlinelibrary.com]

only 3% live cells remained. Compared to *S. aureus*, *E. coli* showed higher susceptibility and sensitivity toward films of PDMAPMA-High QAS.

It can be noted that the kinetics of killing of the films of PDMAPMA-High QAS resembles the results for PDMAPMA-MeI in solution (Fig. 3). A similar mechanism may be proposed here despite the very different physical forms of the polymers in the different cases. In solution, it is proposed that the cell walls of *S. aureus* hinder the diffusion of PDMAPMA to the membrane in a manner similar to the “sieving effect,”³¹ and that the membrane can be efficiently disrupted once the electrostatic forces become sufficient. When used as coatings, because PDMAPMA is immobilized, the polymer cannot diffuse through the cell walls and can only exert a biocidal action through the positive charge at the place where bacteria make contact with the coating. In addition, according to the “phospholipid sponge model” proposed by Bieser and Tiller⁴⁴ and Li et al.,⁴⁵ the antimicrobial polymer coatings irreversibly attract the negatively charged phospholipids and disrupt the membrane of the bacterial cells. Such action can cause strong deformation of the bacteria, as can be seen from the SEM images of the morphologies of bacteria before and after being killed by PDMAPMA-High QAS coating (Fig. 8; additional images are presented in Fig. S8). When acting against *E. coli*, the coating directly contacts the membrane, causing the disruption of the membrane and subsequently the death of the

TABLE 3 The Thicknesses, Degrees of Quaternization, Water Contact Angles, and Surface Streaming Potentials of PDMAPMA Films

Film	Thickness (nm) ^a	Degree of Quaternization (%)	Water Contact Angle (°) ^a	Surface Streaming Potential (mV)
PDMAPMA-Crosslinked	20.6 ± 1.4	7.9	83.8 ± 0.5	-25.0
PDMAPMA-Mid QAS	19.5 ± 0.6	39.8	76.1 ± 0.3	+20.6
PDMAPMA-High QAS	21.9 ± 1.6	80.1	69.6 ± 0.8	+61.8

^a The error is one standard deviation.

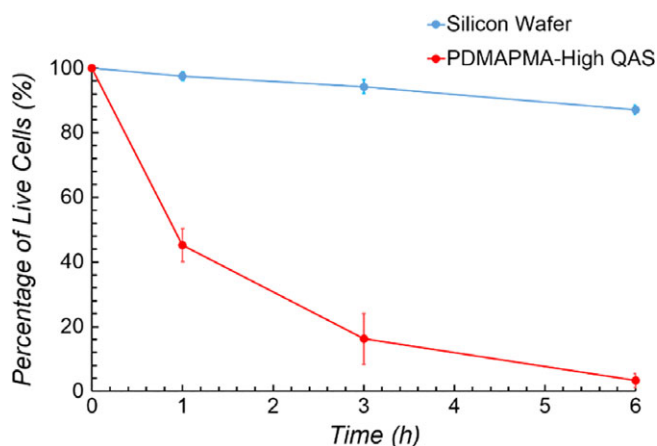


FIGURE 7 The percentage of live *E. coli*, respectively, on silicon wafer and PDMAPMA-High QAS films as the function of incubation time at 1, 3, and 6 h. The error bars ($n = 3$) show one standard deviation. [Color figure can be viewed at wileyonlinelibrary.com]

cells. The thin cell wall between the double lipid layers is not able to mitigate against such strong forces exerted by the coating. The entire surface of the cell is deformed and the cell membrane “collapsed” on the surface of the coating. On the other hand, for *S. aureus*, it is apparent that a “squeezing” effect derived from the electrostatic attraction was exerted on the cell and cytoplasmic substance leaked out of the spherical cell through a crack caused by this force. However, the cationic charge of the coating can only slowly take effect against *S. aureus* as the cell wall shields direct contact with the membrane. As expected for the “phospholipid sponge model,” the biocidal process is therefore slowed.

Relationship between Biocidal Behavior and Charge Density of PDMAPMA Coatings

The three types of films with different degrees of quaternization were incubated with 1×10^6 bacteria in PBS for 6 h.

The relationship between the degree of quaternization of the coatings and the percentage of live cells attached to the coatings is presented in Figure 9. The corresponding fluorescence images of the *S. aureus* and *E. coli* attached to the samples are shown in Figure S9. An increase in the ratio of dead cells can be clearly observed against both strains as the degree of quaternization was increased.

PDMAPMA-Crosslinked films were able to exert an antimicrobial effect against both strains of bacteria, with 61% *S. aureus* and 72% *E. coli* dead. Although the streaming potential of PDMAPMA-Crosslinked film showed a negative surface charge, this only reflects the overall potential difference between the slipping plane and the bulk of dispersive medium. The cationic anilinium groups on the surface can still exert a biocidal effect against bacteria through membrane disruption. The number of accessible cationic groups on the surface of coating was determined by XPS measurements. It also needs to be mentioned that PDMAPMA, with only 7% degree of quaternization, is insoluble in water, and therefore is not able to display biocidal activity through mechanisms of action available to conventional antibiotics, such as inhibition of syntheses of DNA/RNA, cell wall, and proteins,⁴⁶ which require perturbation at the molecular level toward the metabolic pathways. An increase in accessible cationic anilinium groups to 40% led to a reduction of live *S. aureus* and *E. coli* to, respectively, 17 and 9% and a further increase in surface charge rendered more than 90% death of both bacterial strains, with only 3% survival for *E. coli*. Therefore, it can be concluded that higher charge density brings

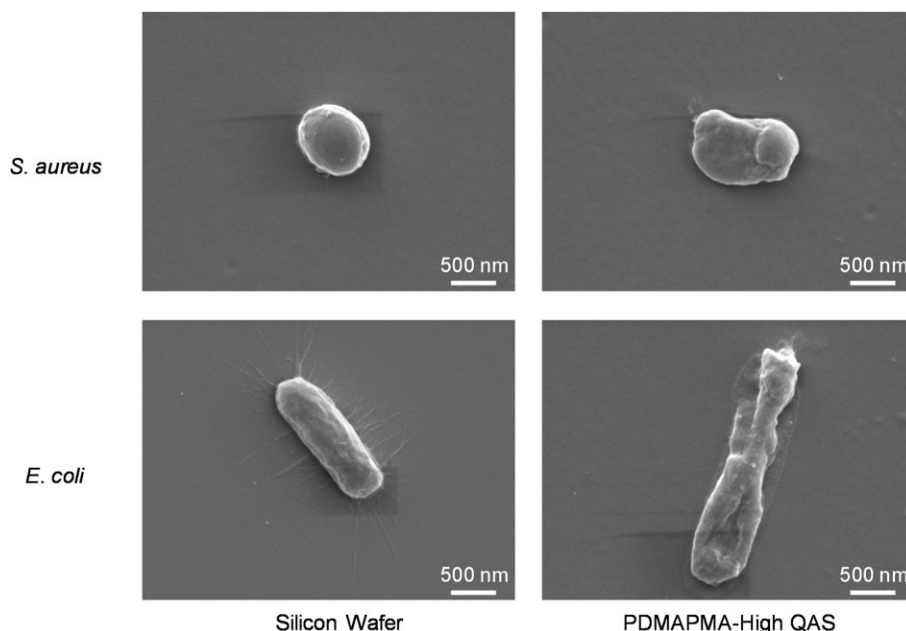


FIGURE 8 The SEM images of bacteria, respectively, on silicon wafer and films of PDMAPMA-High QAS.

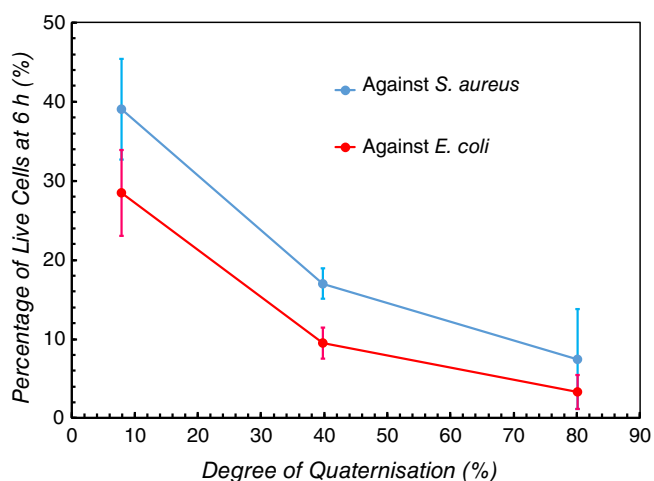


FIGURE 9 The relationship between the biocidal performance at 6 h of incubation and the degree of quaternization of PDMAPMA coatings. The error bars ($n = 3$) show one standard deviation. [Color figure can be viewed at wileyonlinelibrary.com]

more efficient killing of bacteria. This observation is in accordance with the biocidal properties of coatings prepared by grafting of polymers^{39,45} or crosslinking^{44,45} where accessible charge density and the killing efficacy are all positively correlated. In order to reach higher biocidal efficiency and efficacy, increasing the charge density of the coatings appears to be a necessary and effective approach.

Finally, the data in Figure 9 demonstrate that *E. coli* showed shorter survival time against films with the same degree of quaternization. Such an observation is consistent with the differences in killing efficiency of PDMAPMA-High QAS films against the two bacterial strains as discussed in the Synthesis of PDMAPMA Polymer and Polymer Properties section. All of the above information confirms that *E. coli*, compared to *S. aureus*, is more susceptible to charge density and change of charge density, due to its double lipid membrane structure.

CONCLUSIONS

We have shown in this article that quaternized PDMAPMA is an antimicrobial polymeric material with broad biocidal activity. In solution, this polymer showed slightly better inhibition of bacterial growth of *S. aureus* than *E. coli* at lower concentrations, but more efficient biocidal function against *E. coli* at higher concentrations. This behavior may be a consequence of the bulky and rigid structure of the polymer. In addition, the polymer was shown to be nontoxic to human RBCs, but mildly toxic to 3T3 fibroblast cells. MeI-PDMAPMA was then tested as a candidate for antimicrobial polymer coatings and showed strong contact killing action against both *S. aureus* and *E. coli* via disruption of the membrane integrity of bacteria. The influence of charge density in the biocidal films was investigated by adjusting the degree of quaternization of the films. A stronger biocidal effect was achieved for films with higher charge density. We expect that such performance will promote

and broaden the application of polymers with anilinium side functional groups in the biomedical fields.

ACKNOWLEDGMENTS

The authors acknowledge the Australian Research Council (DP130103774, DP140103118, CE140100036, LE110100028, LE140100087, LE160100168, and DP180101221) for funding of this research. The authors also acknowledge the use of equipment managed by the Australian National Fabrication Facility, Queensland Node. The authors would also like to thank The New Zealand Ministry of Business, Innovation and Employment (MBIE) for funding the Biocide Tool Box research programme (UOAX1410).

REFERENCES AND NOTES

- 1 Health Care-Associated Infections Fact Sheet, World Health Organization.
- 2 Review on Antimicrobial Resistance, *Antimicrobial Resistance: Tackling a Crisis for the Health and Wealth of Nations*, 2014.
- 3 X.-Z. Li, H. Nikaido, *Drugs* **2009**, *69*, 1555.
- 4 H. Jenssen, P. Hamill, R. E. W. Hancock, *Clin. Microbiol. Rev.* **2006**, *19*, 491.
- 5 M. Zasloff, *Nature* **2002**, *415*, 389.
- 6 K. A. Brogden, *Nat. Rev. Microbiol.* **2005**, *3*, 238.
- 7 M. S. Ganewatta, C. B. Tang, *Polymer* **2015**, *63*, A1.
- 8 P. Ortega, J. L. Copa-Patino, M. A. Munoz-Fernandez, J. Soliveri, R. Gomez, F. J. de la Mata, *Org. Biomol. Chem.* **2008**, *6*, 3264.
- 9 J. Tolosa, G. Serrano De Las Heras, B. Carrión, T. Segura, P. L. Páez, F. J. de Lera-Garrido, J. Rodríguez-López, J. C. García-Martínez, *ChemistrySelect* **2018**, *3*, 7327.
- 10 J. Clayden, N. Greeves, S. Warren, P. Wothers, *Organic Chemistry*, Oxford University Press: New York, **2001**.
- 11 A. Chen, H. Peng, I. Blakey, A. K. Whittaker, *Polym. Rev.* **2017**, *57*, 276.
- 12 T. A. Sokolova, L. A. Ovsyannikova, *Zh. Obshch. Khim.* **1958**, *28*, 779.
- 13 T. A. Sokolova, L. A. Ovsyannikova, *Bull. Acad. Sci. USSR, Div. Chem. Sci.* **1959**, *8*, 1742.
- 14 F. Li, L. Wang, X. Feng, *Acta Polym. Sin.* **1987**, 144.
- 15 D. J. Liaw, C. C. Huang, *Macromol. Chem. Phys.* **2000**, *201*, 1101.
- 16 D. J. Liaw, C. C. Huang, H. C. Sang, E. T. Kang, *Polymer* **2001**, *42*, 209.
- 17 T. McIlvaine, *J. Biol. Chem.* **1921**, *49*, 183.
- 18 I. Wiegand, K. Hilpert, R. E. W. Hancock, *Nat. Protoc.* **2008**, *3*, 163.
- 19 C. Zhang, S. S. Moonshi, H. Peng, S. Puttick, J. Reid, S. Bernardi, D. J. Searles, A. K. Whittaker, *ACS Sens.* **2016**, *1*, 757.
- 20 T. Ikeda, S. Tazuke, *Macromol. Rapid Commun.* **1983**, *4*, 459.
- 21 C. J. Waschinski, S. Barnert, A. Theobald, R. Schubert, F. Kleinschmidt, A. Hoffmann, K. Saalwächter, J. C. Tiller, *Biomacromolecules* **2008**, *9*, 1764.
- 22 K. A. Gibney, I. Sovadinova, A. I. Lopez, M. Urban, Z. Ridgway, G. A. Caputo, K. Kuroda, *Macromol. Biosci.* **2012**, *12*, 1279.
- 23 R. Tejero, D. López, F. López-Fabal, J. L. Gómez-Garcés, M. Fernández-García, *Biomacromolecules* **2015**, *16*, 1844.
- 24 Z. X. Voo, M. Khan, K. Narayanan, D. Seah, J. L. Hedrick, Y. Y. Yang, *Macromolecules* **2015**, *48*, 1055.

- 25** A. Strassburg, F. Kracke, J. Wengers, A. Jemeljanova, J. Kuepper, H. Petersen, J. C. Tiller, *Macromol. Biosci.* **2015**, *15*, 1710.
- 26** A. Punia, A. Mancuso, P. Banerjee, N. L. Yang, *ACS Macro Lett.* **2015**, *4*, 426.
- 27** R. Tejero, B. Gutierrez, D. Lopez, F. Lopez-Fabal, J. L. Gomez-Garces, M. Fernandez-Garcia, *Acta Biomater.* **2015**, *25*, 86.
- 28** T. Ikeda, S. Tazuke, M. Watanabe, *Biochim. Biophys. Acta* **1983**, *735*, 380.
- 29** T. Ikeda, H. Yamaguchi, S. Tazuke, *Antimicrob. Agents Chemother.* **1984**, *26*, 139.
- 30** Y. Qiao, C. Yang, D. J. Coady, Z. Y. Ong, J. L. Hedrick, Y. Y. Yang, *Biomaterials* **2012**, *33*, 1146.
- 31** K. Lienkamp, A. E. Madkour, K. N. Kumar, K. Nusslein, G. N. Tew, *Chem. A Eur. J.* **2009**, *15*, 11715.
- 32** L. Asri, M. Crismaru, S. Roest, Y. Chen, O. Ivashenko, P. Rudolf, J. C. Tiller, H. C. van der Mei, T. J. A. Loontjens, H. J. Busscher, *Adv. Funct. Mater.* **2014**, *24*, 346.
- 33** D. Fischer, Y. Li, B. Ahlemeyer, J. Krieglstein, T. Kissel, *Biomaterials* **2003**, *24*, 1121.
- 34** W. Chin, C. Yang, V. W. L. Ng, Y. Huang, J. Cheng, Y. W. Tong, D. J. Coady, W. Fan, J. L. Hedrick, Y. Y. Yang, *Macromolecules* **2013**, *46*, 8797.
- 35** K. Kuroda, W. F. DeGrado, *J. Am. Chem. Soc.* **2005**, *127*, 4128.
- 36** E. F. Palermo, K. Kuroda, *Biomacromolecules* **2009**, *10*, 1416.
- 37** Z. K. Xu, Y. F. Yang, L. S. Wan China Patent CN101254418, March 9, **2008**.
- 38** G. Gozzelino, C. Lisanti, S. Beneventi, *Colloids Surf. A* **2013**, *430*, 21.
- 39** R. Kugler, O. Bouloussa, F. Rondelez, *Microbiology* **2005**, *151*, 1341.
- 40** B. C. Allison, B. M. Applegate, J. P. Youngblood, *Biomacromolecules* **2007**, *8*, 2995.
- 41** A. D. Fuchs, J. C. Tiller, *Angew. Chem. Int. Ed.* **2006**, *45*, 6759.
- 42** L. A. B. Rawlinson, S. M. Ryan, G. Mantovani, J. A. Syrett, D. M. Haddleton, D. J. Brayden, *Biomacromolecules* **2010**, *11*, 443.
- 43** M. E. Olson, H. Ceri, D. W. Morck, A. G. Buret, R. R. Read, *Can. J. Comp. Med.* **2002**, *66*, 86.
- 44** A. M. Bieser, J. C. Tiller, *Macromol. Biosci.* **2011**, *11*, 526.
- 45** P. Li, Y. F. Poon, W. F. Li, H. Y. Zhu, S. H. Yeap, Y. Cao, X. B. Qi, C. C. Zhou, M. Lamrani, R. W. Beuerman, E. T. Kang, Y. G. Mu, C. M. Li, M. W. Chang, S. S. J. Leong, M. B. Chan-Park, *Nat. Mater.* **2011**, *10*, 149.
- 46** M. A. Kohanski, D. J. Dwyer, J. J. Collins, *Nat. Rev. Microbiol.* **2010**, *8*, 423.